Technical and Software Improvements of the EPR Spectroscopy Endstation at the NovoFEL Facility: Status 2020

Anatoly R. Melnikov[1,2,3,a)], Mikhail A. Kiskin[4], Yaroslav V. Getmanov[3,5], Oleg A. Shevchenko[5], Matvey V. Fedin[2,3], Sergey L. Veber[2,3]

[1]*Voevodsky Institute of Chemical Kinetics and Combustion of the Siberian Branch of the Russian Academy of Sciences, 630090 Novosibirsk, 3, Institutskaya Str., Russia*
[2]*International Tomography Center of the Siberian Branch of the Russian Academy of Sciences, 630090 Novosibirsk, 3a, Institutskaya Str., Russia*
[3]*Novosibirsk State University, 630090 Novosibirsk, 1, Pirogova Str., Russia*
[4]*Kurnakov Institute of General and Inorganic Chemistry of the Russian Academy of Sciences, 119991 Moscow, 31, Leninsky Ave., Russia*
[5]*Budker Institute of Nuclear Physics of the Siberian Branch of the Russian Academy of Sciences, 630090 Novosibirsk, 11, Acad. Lavrentieva Ave., Russia*

[a)]Corresponding author: anatoly.melnikov@tomo.nsc.ru

Abstract The X-band Electron Paramagnetic Resonance (EPR) spectroscopy endstation at the Novosibirsk Free Electron Laser (NovoFEL) facility is capable for steady-state (CW) EPR and time-resolved (TR) continuous wave EPR experiments. Recently several upgrades in experimental hardware and software have been done, aiming to more productively use the time of an experimental session and to increase the control of experimental parameters during the session. Firstly, we installed detectors with different time resolution for tracking radiation produced by NovoFEL. Secondly, on the basic of fsc2 program, we implemented a possibility of simultaneous use of two oscilloscopes, configured at different timescale and/or sensitivity. Finally, we developed software for on-the-fly CW and TR experimental data viewing and treatment.

INTRODUCTION

The Novosibirsk Free Electron Laser (NovoFEL) facility consists of three free electron lasers (FELs) that produces high-power tunable laser radiation in mid-infrared (~1100 cm^{-1}), far-infrared (~200 cm^{-1}), and terahertz (~40 cm^{-1}) frequency ranges [1, 2], for uniformity hereinafter referred to as the terahertz (THz) radiation. NovoFEL operates in quasi-continuous (CW) mode and produces a periodic train of radiation pulses with several tens of picoseconds duration. Recently a possibility of macropulse generation was implemented using an electronic modulation system [3]. Macropulses contain the sequence of individual picoseconds pulses and can have almost any desired duration. The NovoFEL facility is equipped with a number of endstations devoting to various experimental techniques [1]. One of them, the X-band EPR spectroscopy endstation, allows investigation of paramagnetic species in various media using continuous wave (CW) and time-resolved (TR) EPR techniques [4-10]. During last year, several useful upgrades of experimental hardware and software have been done at the EPR endstation. Improvements include implementations of fast detectors for recording the THz macropulses during experiment, possibility of simultaneous use of two oscilloscopes, configured at different sensitivity and/or timescale, and the development of software for experimental data viewing and treatment. The main part of the manuscript is divided into two sections. The first section discusses hardware upgrades of the endstation. The discussion consists of an example of the simultaneous use of two oscilloscopes in TR EPR experiment, as well as possible positions

and time resolution of available THz detectors. The second section describes the developed software. The software was written in Wolfram Mathematica (WM) [11]. It includes a simple graphical user interface (GUI) which allows the interaction with the program without knowledge of Wolfram Language.

RECENT ADVANCES IN HARDWARE AND SOFTWARE OF THE NOVOFEL EPR SPECTROSCOPY ENDSTATION

Hardware Improvements of the Endstation

Simultaneous Use of Two Oscilloscopes

Large scale facilities like NovoFEL offer possibilities for carrying out different types of experiments under unique conditions. Since they typically work as core facilities centers, time of experimental session is limited. In such conditions automatization of experiments and measuring as much data as possible per unit of time is of great importance. To automatize measurements and have possibility to easily adapt to different hardware, an open-source fsc2 program [12] is used as the main program for controlling spectrometer at the EPR endstation of NovoFEL. This program employs modular approach to the handling of devices that allows using new devices by writing modules for them in C programming language.

As it was mentioned in introduction, the EPR spectroscopy endstation can be used for measuring CW and TR EPR spectra. The TR EPR spectroscopy is sensitive to transient processes and able to trace a change in microwave (MW) absorption caused by an external influence such as laser pulse or THz macropulse. The shape and temporal evolution of the detected signal is determined by the sample under study and can have distinctive behavior and amplitude during the THz macropulse and at longer timescale where the kinetics is typically determined by relaxation processes. Recording of the transient signal kinetics is typically carried out by oscilloscopes. To improve the efficiency of experimental sessions, it is reasonable to use two oscilloscopes simultaneously that have settings (timescale and sensitivity) optimized for detection of the signals with distinctive characteristics. This opportunity was implemented using fsc2 program for which a new module for Keysight oscilloscope was written. Oscilloscopes are connected to computer via VXI-11 protocol. Figure 1 shows the current scheme of the device network that is controlled by computer.

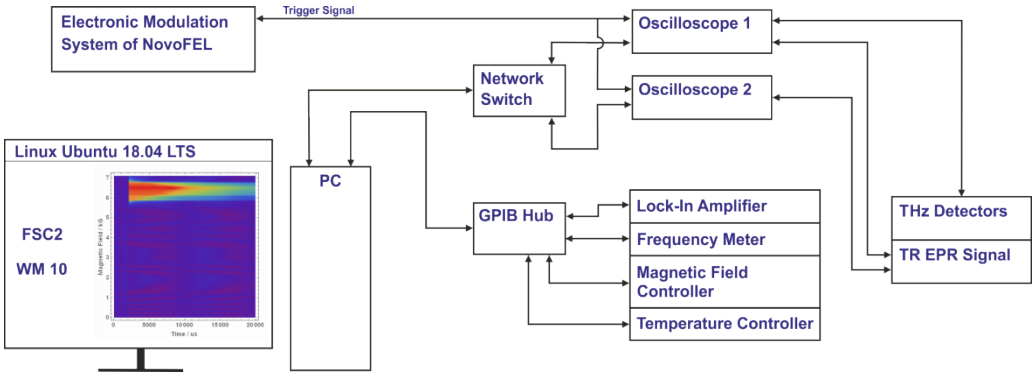

FIGURE 1. General scheme of the control computer (PC) with the network of ethernet and GPIB devices. Oscilloscopes are synchronized with electron beam [3].

Figure 2 shows a two-dimensional TR EPR spectrum as well as its magnetic field and time cross-sections for diamagnetically diluted $[Co_{0.01}Zn_{0.99}(piv)_2(2\text{-}NH_2\text{-}Py)_2]$ complex measured under pulsed THz radiation with pulse duration of 100 μs and wavenumber of 41.7 cm^{-1}. To eliminate the background signal, TR EPR signal was accumulated at off-resonance magnetic-field position (background) and subtracted from those recorded on resonance. The spectrum was obtained at cryogenic temperature from a single crystal of $[Co_{0.01}Zn_{0.99}(piv)_2(2\text{-}NH_2\text{-}Py)_2]$ in which cobalt is a paramagnetic ion and piv is anion of trimethylacetic acid. The complex was synthesized similarly to complex $[Co(piv)_2(2\text{-}NH_2\text{-}Py)_2]$ [13] using a mixture of $[Co(piv)_2]_n$ and $[Zn(piv)_2]_n$ in a ratio of 1:99. Detailed description of experimental setup can be found elsewhere [3, 4].

A strong positive signal in the range of 500 – 700 mT of Fig. 2 originates from the cobalt complex and is caused by the sample heating due to the THz radiation absorption. The sample temperature change leads to the change in the population of spin levels that manifests itself as a strong T-jump signal in the TR EPR spectrum [4].

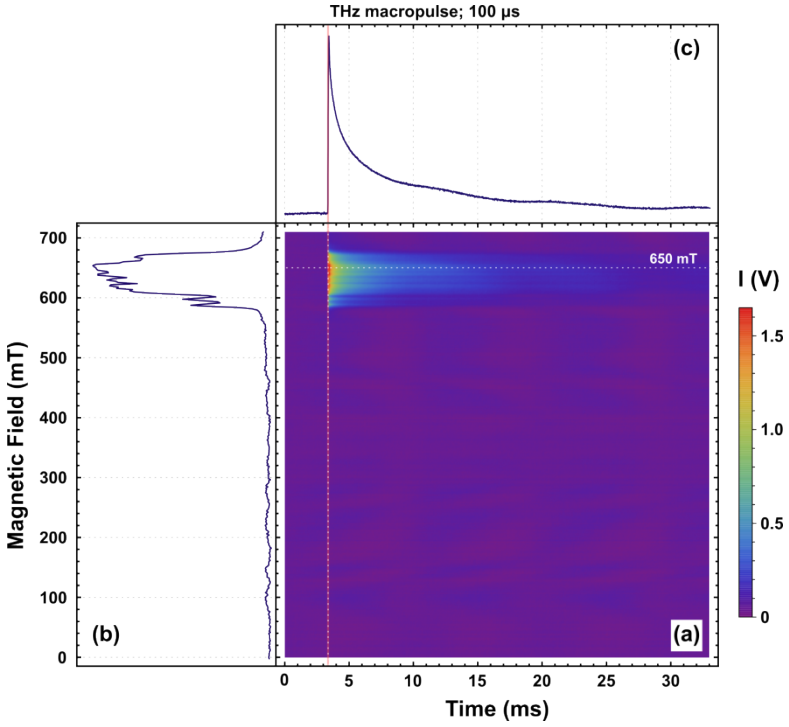

FIGURE 2. (a) Two-dimensional time-resolved EPR spectrum of a single crystal of $[Co_{0.01}Zn_{0.99}(piv)_2(2\text{-}NH_2\text{-}Py)_2]$. Temperature is 4.7 K, microwave frequency is 9.76 GHz, microwave power is 2 mW, THz radiation pulse length is 100 µs, repetition rate is 10 Hz, wavenumber is 41.7 cm^{-1}. The complex was irradiated with THz radiation in the time interval that is highlighted by a pink rectangle in the kinetics shown in (c). The orientation of the single crystal corresponds to the stationary EPR spectrum shown in Fig. 3. (b) The field profile of the TR signal at the time point of 3.46 ms (the signal maximum, shown in (a) by the white dashed line). (c) The kinetics of the TR signal in magnetic field of 650 mT (shown in (a) by the white dashed line).

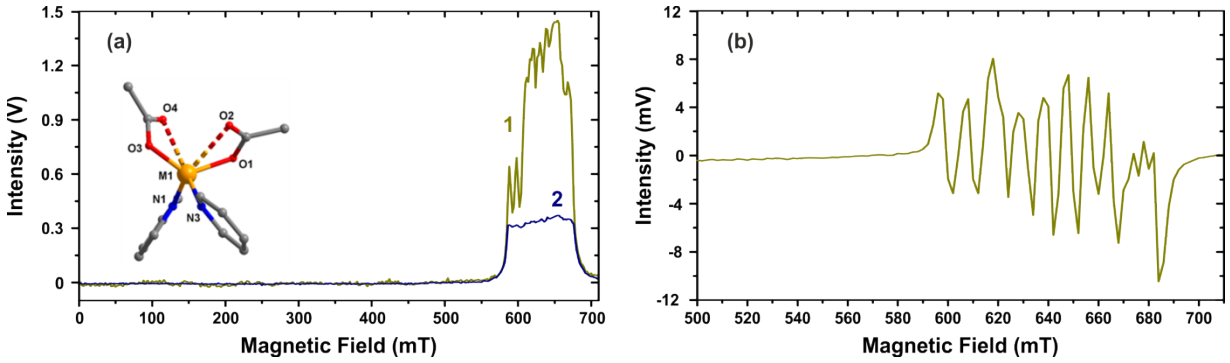

FIGURE 3. (a) Magnetic field cross-sections of TR EPR spectrum of $[Co_{0.01}Zn_{0.99}(piv)_2(2\text{-}NH_2\text{-}Py)_2]$ after the THz macropulse measured simultaneously at two oscilloscopes with different sensitivity: **1** – 500 mV, **2** – 30 mV. Temperature is 4.7 K, microwave frequency is 9.76 GHz, microwave power is 2 mW, THz radiation pulse length is 100 µs, repetition rate is 10 Hz, wavenumber is 41.7 cm^{-1}. The inset shows structural formula of $[Co(piv)_2(2\text{-}NH_2\text{-}Py)_2]$ where methyl groups in pivalate, amino group and H atoms in 2-aminopyridine are omitted for clarity. (b) CW EPR spectrum of $[Co_{0.01}Zn_{0.99}(piv)_2(2\text{-}NH_2\text{-}Py)_2]$ measured at 5.3 K. MW frequency is 9.76 GHz, MW power is 20 µW, modulation amplitude is 0.3 mT, modulation frequency is 100 kHz, time constant is 30 ms.

An example of the use of two oscilloscopes is given in Fig 3a. This figure demonstrates magnetic field cross-sections of TR EPR signals obtained for $[Co_{0.01}Zn_{0.99}(piv)_2(2\text{-}NH_2\text{-}Py)_2]$ by the simultaneous use of two Keysight DSOX2012A (Keysight Technologies, USA) oscilloscopes with different sensitivity. As it can be seen from Fig. 3a, the magnetic field range of detected TR signal coincides with the range of CW EPR spectrum for the same crystal orientation shown in Fig. 3b. In the used settings the first oscilloscope detects the main signal, while the second, being off the scale in the range of the main signal, can be used for detection of a smaller in amplitude signal in a different magnetic field region. Alternatively, two oscilloscopes tuned at different timescale can be used for simultaneous tracking fast dynamics of TR signal at the THz pulse timescale and subsequent relaxation of the signal at a longer time.

Detectors for Tracking THz Radiation

Controlling the shape and duration of THz macropulse during or between experiments is crucial for measuring TR EPR spectrum under THz radiation. At the moment, the EPR spectroscopy endstation has three available THz detectors with different sensitivity and time resolution. Figure 4a schematically shows the optical system of the endstation and possible positions of detectors.

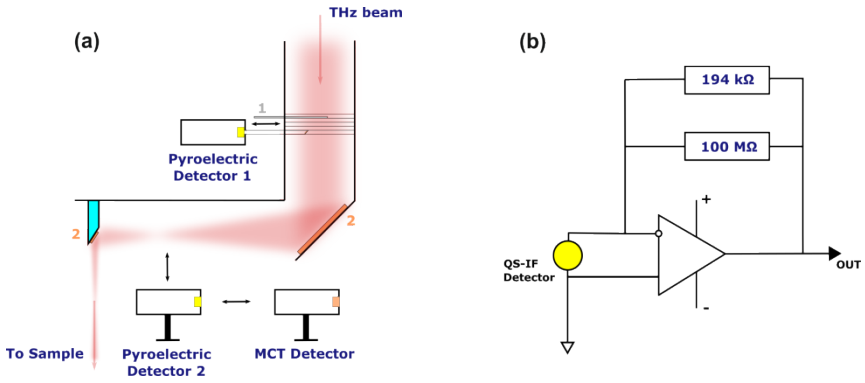

FIGURE 4. (a) Layout of various THz detectors at the EPR spectroscopy endstation. Numbers show: **1** – movable mechanical shutter, **2** – off-axis parabolic mirrors. Detectors can be placed directly at the focus of the first mirror (pyroelectric detector 2 or MCT detector) or used to control the duration of THz macropulses during experiment (pyroelectric detector 1). (b) Circuit diagram of pyroelectric detector 2 with the modified feedback resistor to improve the time resolution.

The first detector is pyroelectric detector Gentec QS-IF5 (Gentec EO, Canada) in the default configuration that is attached to a movable hollow copper tube, beveled at 45 degrees to the incident THz beam from one side. Such tube plays a role of a mirror and reflects a small part of radiation on the detector, which allows tracking THz macropulses during experiment. The tube does not significantly affect the total THz radiation power, since it is located before the first focusing element of the optical system. Figure 5a shows an example of THz macropulse measured by this detector using Keysight DSOX3034T (Keysight Technologies, USA) oscilloscope. The estimated time resolution of the first detector is 2.5 ms, according to the long tail after THz pulse.

The second detector is the same pyroelectric detector Gentec QS-IF5 in which a feedback resistor was installed to improve the time resolution. Circuit diagram of the second detector is shown in Fig. 4b. Since the performed modification at the same time decreases sensitivity, this detector should be placed after the first focusing element of the optical system as it is shown in Fig 4a. Figure 5b shows an example of THz macropulse measured by this detector. Using Fig. 5c, the time resolution of the second detector can be estimated as 300 ns. This is already enough to roughly resolve a fine structure of NovoFEL radiation, consisting of a train of individual THz pulses with ~10-70 ps duration [4]. Pyroelectric detectors have a wide spectral sensitivity and can be used for all three FELs available at NovoFEL facility. In addition to them, mercury-cadmium-telluride (MCT) LN_2 detector (InfraRed Associates, USA) can be used in the mid-infrared frequency range of the third FEL. Due to geometric constraints the MCT detector can be placed only after the first focusing element similar to the second detector. An example of macropulse measured by MCT detector at 1125 cm^{-1} wavelength can be found in ref. [3]. The estimated time resolution of the third detector is 200 ns.

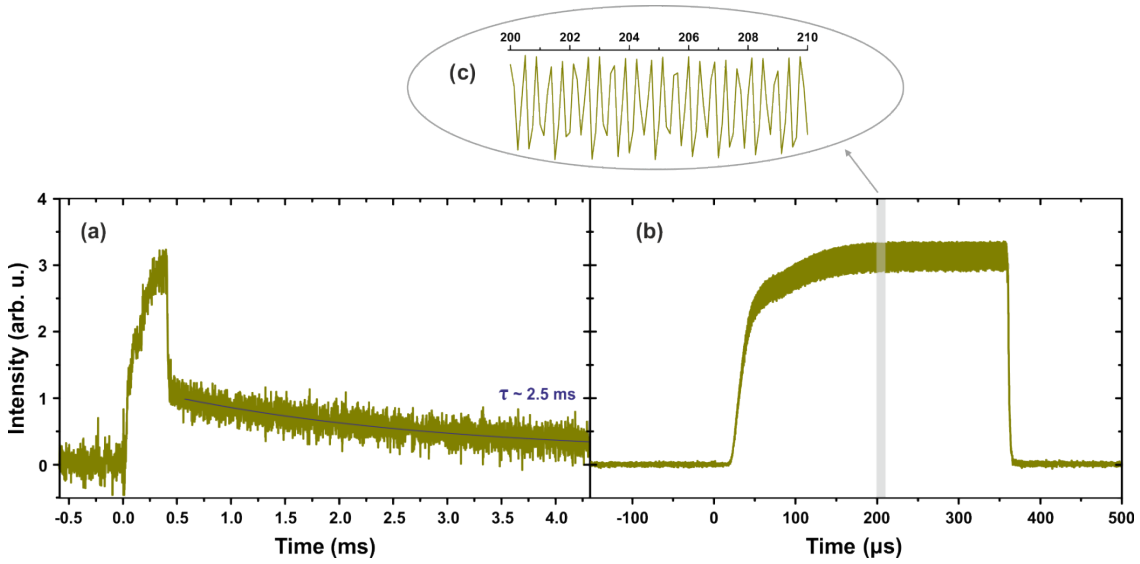

FIGURE 5. (a) Example of THz macropulse with 400 μs duration registered by pyroelectric detector 1 at 76.9 cm^{-1}. Dark blue line shows the result of one exponential fitting by the model $a + b \cdot \exp(-t/\tau)$ with τ equals to 2.5 ms. (b) The same for 350 μs macropulse registered by pyroelectric detector 2. (c) A closer view of (b) in the range of 10 μs with visible fine structure of the macropulse (limited by time resolution of the detector).

Development of Software for Experimental Data Treatment

Fsc2 is a versatile and flexible program for controlling spectrometers with a good graphical user interface that allows visualizing raw 2D and 1D data during experiment. At the moment, in this program there is no way to open previously saved data. The possibility of opening saved data directly on spectrometer for on-the-fly treatment is useful at large scale facilities where experimental time is limited. At the EPR spectroscopy endstation this possibility was realized using Wolfram Mathematica. At the core of the program lies the concept of dynamic visualization using Manipulators and Dynamic Modules of Wolfram Language. The program has internal WM graphical user interface for all realized features. Several screenshots of GUI are shown in Fig. 6.

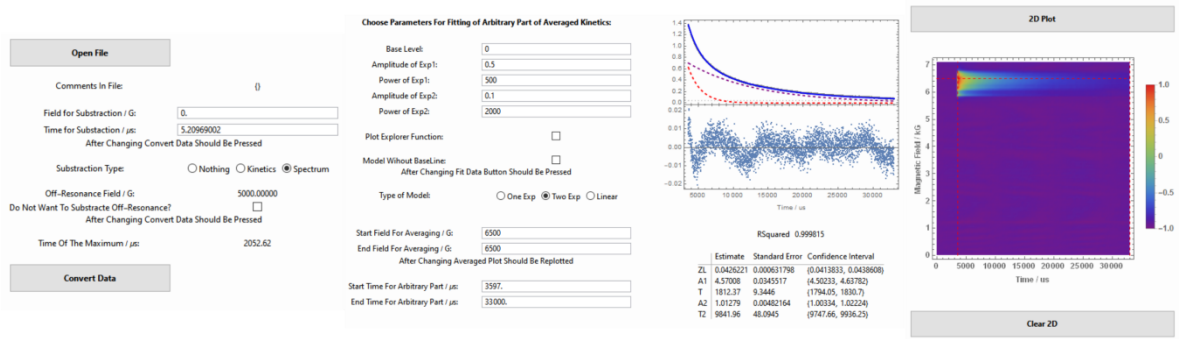

FIGURE 6. Examples of graphical user interface of WM program for experimental data visualization and treatment that is used at the EPR spectroscopy endstation at NovoFEL.

Currently the program enables a number of basic manipulations with raw experimental data, such as baseline correction, normalization, plotting, *etc*. Plotting functions include 1D magnetic field and time cross-sections of time-resolved EPR spectrum with the possibility of averaging in the desired time or magnetic field range, and 2D density plot. Least squares fitting is available in an arbitrary chosen timespan using one or two exponential function

as a model. All functions are realized using simple GUI that allows interacting with the program without knowledge of Wolfram Language. The source code can be found at https://github.com/Anatoly1010/TR_EPR.

CONCLUSION

In this work, we describe recent advances in experimental hardware and software at the X-band EPR endstation of the NovoFEL facility. There are three main improvements that help to increase the efficiency of an experimental session and improve the control of experimental parameters during the session. The first upgrade is the implementation of three detectors with different time resolution and sensitivity that allows recording the THz macropulses during experiment. The second is the realization of the possibility of simultaneous use of two oscilloscopes, configured at different timescale and/or sensitivity. Finally, special software for CW and TR experimental data viewing and treatment was developed using Wolfram Mathematica. All the improvements allow spending experimental time more productively and carrying out experiments at a higher technical and software level.

ACKNOLEDGMENTS

Modification of hardware and software of the EPR spectroscopy endstation at NovoFEL facility was funded by the Russian Science Foundation, grant number 17-13-01412. Synthesis of $[Co_{0.01}Zn_{0.99}(piv)_2(2\text{-}NH_2\text{-}Py)_2]$ complex was funded by IGIC RAS state assignment. The authors are grateful to D. V. Ogorodnikov and S. A. Babin for their help in creating the fsc2 module for Keysight oscilloscope.

REFERENCES

1. G. N. Kulipanov, E. G. Bagryanskaya, E. N. Chesnokov, Y. Y. Choporova, V. V. Gerasimov, Y. V. Getmanov, S. L. Kiselev, B. A. Knyazev, V. V. Kubarev, S. E. Peltek, V. M. Popik, T. V. Salikova, M. A. Scheglov, S. S. Seredniakov, O. A. Shevchenko, A. N. Skrinsky, S. L. Veber, and N. A. Vinokurov, IEEE T. THz Sci. Techn. **5 (5)**, 798-809 (2015).
2. O. A. Shevchenko, V. S. Arbuzov, N. A. Vinokurov, P. D. Vobly, V. N. Volkov, Y. V. Getmanov, Y. I. Gorbachev, I. V. Davidyuk, O. I. Deychuly, E. N. Dementyev, B. A. Dovzhenko, B. A. Knyazev, E. I. Kolobanov, A. A. Kondakov, V. R. Kozak, E. V. Kozyrev, V. V. Kubarev, G. N. Kulipanov, E. A. Kuper, I. V. Kuptsov, G. Y. Kurkin, S. A. Krutikhin, L. E. Medvedev, S. V. Motygin, V. K. Ovchar, V. N. Osipov, V. M. Petrov, A. M. Pilan, V. M. Popik, V. V. Repkov, T. V. Salikova, I. K. Sedlyarov, S. S. Serednyakov, A. N. Skrinsky, S. V. Tararyshkin, A. G. Tribendis, V. G. Tcheskidov, K. N. Chernov, and M. A. Scheglov, Phys. Procedia **84**, 13-18 (2016).
3. O. A. Shevchenko, A. R. Melnikov, S. V. Tararyshkin, Y. V. Getmanov, S. S. Serednyakov, E. V. Bykov, V. V. Kubarev, M. V. Fedin, and S. L. Veber, Materials **12 (19)**, 3063 (2019).
4. S. L. Veber, S. V. Tumanov, E. Y. Fursova, O. A. Shevchenko, Y. V. Getmanov, M. A. Scheglov, V. V. Kubarev, D. A. Shevchenko, I. I. Gorbachev, T. V. Salikova, G. N. Kulipanov, V. I. Ovcharenko, and M. V. Fedin, J. Magn. Reson. **288**, 11-22 (2018).
5. L. Kevan and M.K. Bowman, *Modern Pulsed and Continuous-Wave Electron Spin Resonance* (John Wiley and Sons, New York, USA, 1990), p. 440.
6. A. Est, eMagRes, **5**, 1411-1422 (2016).
7. G. R. Eaton and S. S Eaton, eMagRes, **5**, 1529-1542 (2016).
8. M. D. E. Forbes, L. E. Jarocha, S. Sim, and V. F. Tarasov, in *Advances in Physical Organic Chemistry,* edited by I. H. Williams and N. H. Williams (Academic Pres, London, UK, 2013), **47**, p. 1-83.
9. A. Schnegg, eMagRes, **6**, 115-132 (2017).
10. S. Weber, eMagRes, **6**, 255-270 (2017).
11. Wolfram Mathematica, https://www.wolfram.com/mathematica/.
12. J. T. Törring, https://www.fsc2.org/.
13. N. A. Bokach, V. Yu. Kukushkin, M. Haukka, T. B. Mikhailova, A. A. Sidorov, and I. L. Eremenko, Russ. Chem. Bull. **55** (**1**), 36-43 (2006).